



Univerzita Komenského v Bratislave  
Fakulta matematiky, fyziky a informatiky



**RNDr. Alžbeta Holúbeková**

**Autoreferát dizertačnej práce**

Theoretical study of coumarin derivatives in the inclusion complexes with  $\beta$ -cyclodextrin and in the solution

**na získanie akademického titulu philosophiae doctor**

**v odbore doktorandského štúdia: 4.1.11 Chemická fyzika**

**Bratislava, 2012**

**Dizertačná práca bola vypracovaná v dennej forme doktorandského štúdia na Katedre jadrovej fyziky a biofyziky.**

**Predkladateľ:** RNDr. Alžbeta Holúbeková  
Katedra jadrovej fyziky a biofyziky  
Mlynská dolina – pavilón F1  
842 48 Bratislava 4

**Školiteľ:** prof. RNDr. Ján Urban, DrSc.  
Katedra jadrovej fyziky a biofyziky  
Mlynská dolina – pavilón F1  
842 48 Bratislava 4

**Oponenti:** prof. Ing. Ondrej Kysel', CSc.  
Katedra chémie  
Fakulta prírodných vied  
Univerzita Mateja Bela  
Tajovského 40  
974 01 Banská Bystrica  
e-mail: ondrej.kysel1@gmail.com  
tel: 048 4467353

doc. Pavel Neogrády, Dr.  
Katedra fyzikálnej chémie a teoretickej chémie  
Prír.F UK, Mlynská dolina CH1  
842 15 Bratislava  
e-mail: pavel.neogrady@fns.uniba.sk  
tel: 02 60296691

prof. Ing. Jaroslav Burda, DrSc.  
Matematicko-fyzikální fakulta  
Univerzita Karlova v Praze  
Ke Karlovu 3  
121 16 Praha 2, Česká republika  
e-mail: burda@karlov.mff.cuni.cz  
tel: 00420-2-2191-1246

**Obhajoba dizertačnej práce sa koná: .....**

**pred komisiou pre obhajobu dizertačnej práce v odbore doktorandského štúdia 4.1.11 Chemická fyzika**

**vymenovanou predsedom odborovej komisie dňa .....**

**na .....**

.....

**Predseda odborovej komisie:**

prof. RNDr. Ján Urban, DrSc.  
Katedra jadrovej fyziky a biofyziky  
Mlynská dolina – pavilón F1  
842 48 Bratislava 4

# 1 Introduction

Theoretical studies present an important contribution to the knowledge of the physical processes at molecular level. Information on molecular and electronic structure, absolute and relative energies, interactions with other molecules, excited state properties, dipole moments and many others can be obtained by computer simulation. Methods used to calculate properties of interest range from early very approximate to high accurate quantum methods. Among the most popular and versatile methods available in computational physics and chemistry is the density functional theory (DFT) and its time-dependent extension the time dependent density functional theory (TD DFT). The main advantages of DFT (and TD DFT) are its computational efficiency and versatility due to a number of exchange-correlation functionals suitable for almost every field of interest. Moreover, further development of new functionals is current research topic. DFT and TD DFT cover a wide area of properties of interest like molecular structures, vibrational frequencies, relative energies (atomic energies, atomization energies, ionization energies, electron affinities), excitation and deexcitation energies, electric and magnetic properties (dipole moments, polarizabilities). DFT can be also very useful in estimation of host-guest complex geometries and for complexation energy calculations.

The theoretical research in supramolecular assemblies is important part of chemistry, molecular biology and pharmacy. Complexes can be formed by encapsulation of appropriate guest molecule in the cavity of macrocyclic host molecule. A variety of possible host molecules is known. Cyclodextrins present an ideal host molecule due to their availability, varying size of the cavity depending on the number of glucose units involved and ability to form hydrogen bonds to the guests. Therefore, they can encapsulate a wide variety of guest molecules. Complexes of  $\beta$ -cyclodextrin and chromophores are studied to develop chemical sensors. Among the suitable chromophores are coumarins because of their high fluorescence quantum yield. Properties of specific coumarin derivative depend on its substituent groups. Additionally, some coumarins present an ideal solvatochromic probe like, for instance, coumarin 153. It is a rigid molecule, significant change in dipole moment occurs upon its excitation, the first excited state of c153 is not contaminated from other excited states and it shows significant red shift depending on the polarity of solvent environment.

## 1.1 Aim of thesis

The primary objective of presented dissertation thesis is to offer a comprehensive picture of structural and spectral properties of selected coumarin derivatives in the gas phase, in the solution and in the complexes with  $\beta$ -cyclodextrin. Following steps were performed in order to fulfil this goal.

1. Optimization of gas-phase structures of coumarins and  $\beta$ CD-coumarin inclusion complexes. Comparison of geometries and complexation energies calculated at semiempirical and DFT level of theory. Spectra calculation on obtained structures and estimation of the shift due to the complex formation.
2. TD DFT benchmark study on coumarin 153 in various solvents. Calculation of spectral characteristics, estimation of ground and excited state dipole moments. Comparison to experimental results.
3. The evaluation of spectral characteristics of coumarin 47, including absorption spectra, emission spectra, solvatochromic shift and Stokes shift. Calculation of ground and excited state dipole moment at various levels of theory.
4. Proposal of cavity model of  $\beta$ CD-coumarin 47 complex in water. Calculation of absorption maxima and ground and excited state dipole moment difference using cavity model. Estimation of various contributions to overall shift after encapsulation of coumarin 47 in  $\beta$ CD.

## 1.2 Computational details

Principally, the calculations have been performed with the GAUSSIAN03 suite of programs [1] applying default procedures and parameters. For the visualization and interpretation of obtained data programs Molden 7 and Mercury 1.4.2 have been used. The  $\beta$ CD (Fig. 1) input structure for the calculation was taken from the Cambridge Crystallographic Database [2]. The structures of coumarin 6, 30, 47, 522 (Fig. 2) were constructed using Hyperchem code [3]. Each molecule was optimized at the PM3 [4,5] level of theory with various geometries of substituents. The one with lowest energy was chosen to build the complex with  $\beta$ CD. The input structure of the  $\beta$ CD-coumarin complex was formed by the following way:  $\beta$ CD was placed at the origin of a coordinate system and coumarin was put on the edge of secondary rim and passed through the cavity by steps. The step length was 0,1 Å. In each step four angles were optimized which characterize the relative position of coumarin and  $\beta$ CD. The

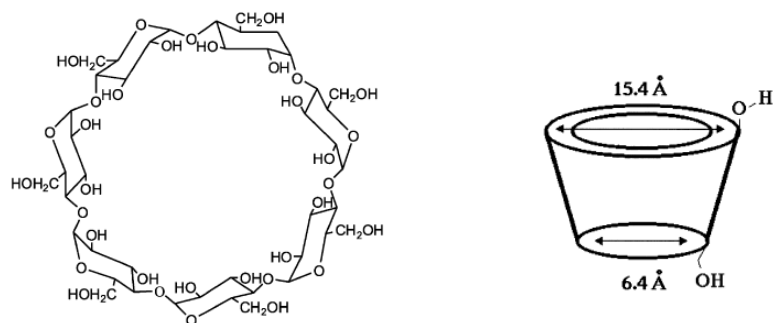


Fig. 1 Structure and topology of  $\beta$ -cyclodextrin molecule

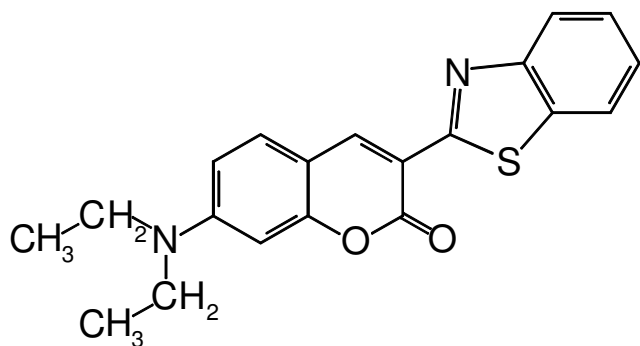


Fig. 2a Coumarin 6

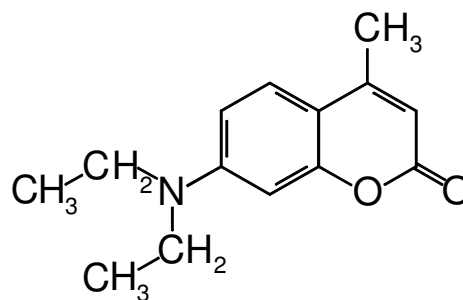


Fig. 2b Coumarin 47

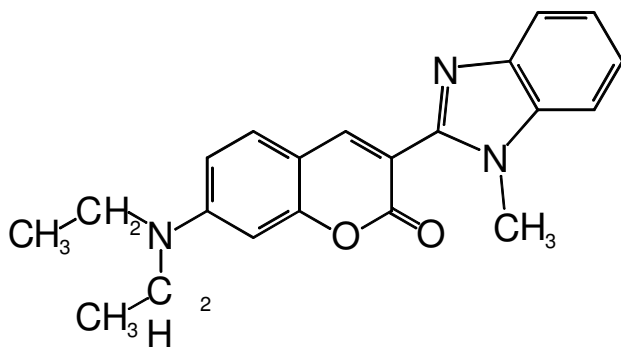


Fig. 2c Coumarin 30

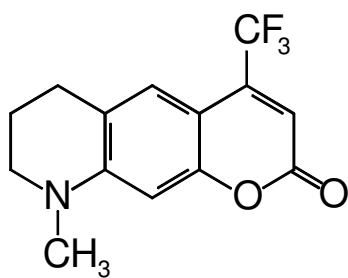


Fig. 2d Coumarin 522

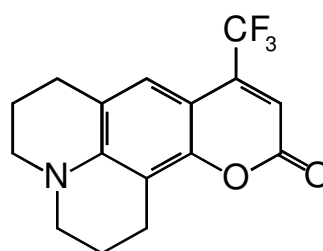


Fig. 2e Coumarin 153

same was carried out with the coumarin entering the cavity from the opposite side. After that the lowest energy conformation was optimized without any restrictions. The with PM3 method previously fully optimized complexes were used for the calculations at the DFT level of theory (HCTH method [6]) using 6-31G basis set. In the first step the relative position of coumarin and  $\beta$ CD was optimized. Afterwards full optimization of the supramolecular system was performed.

The gas phase geometries of coumarins were optimized at PM3 and DFT levels. Various functionals (HCTH [6], PBE0 [7] and B3LYP [8-10]) with two different basis sets (6-31G and 6-31+G(d,p)) were used for the minimizations.

Complexation energy  $\Delta E = E_{complex} - (E_{\beta CD} + E_{coumarin})$  was estimated for the optimized complexes.

To see the influence of complex formation on spectra the absorption maxima of coumarins and  $\beta$ CD-coumarin complexes were estimated. Calculations were carried out at different levels of theory: CIS/6-31G, HCTH/6-31G, PBE0/6-31G. Additionally, we performed the spectra calculation on B3LYP/6-31+G(d,p) optimized structures of coumarins at PBE0/TZVPP, PBE0/6-31+G(d,p) levels of theory. For the two smaller molecules (c47 and c522) we evaluated the spectra at CC2/ aug-cc-pvDZ and CC2/def2-TZVPP levels of theory.

The principal method for calculation of spectral properties of coumarin 153 and 47 molecules was TD PBE0. The spectra calculations in this section were performed on B3LYP/6-31+G(d,p) ground state gas-phase geometry. To consider the solvent effects, the polarizable continuum model (PCM) was applied [11]. Spectra in vacuum were evaluated at following levels of theory: PBE0/6-31+G(d,p), PBE0/def2-TZVPP, CC2/aug-cc-pvDZ and CC2/def2-TZVPP.

The absorption maxima computed in the presence of the solvent reaction field have been determined by using the non-equilibrium solutions with two different basis sets 6-31+G(d,p) and def2-TZVPP. Consequently the solvatochromic shift of coumarin in the solvents was calculated. To enable the comparison of theoretical and experimental values the shift from cyclohexane instead of the gas-to-solution shift was estimated. To evaluate the dynamic Stokes shift calculation of excitation energies in solvents have been performed within the equilibrium approximation. The difference between excitation energies calculated by using the non-equilibrium and equilibrium solutions provided a measure of dynamic Stokes shift. Ground state and excited state dipole moments were estimated at different levels of theory: CIS/6-31+G(d,p) , TD PBE0/6-31+G(d,p) and CC2/aug-cc-pvDZ. Since the excited

state dipole moment evaluation is not directly included in GAUSSIAN03, these calculations were carried out using GAUSSIAN09.

In general, the same approach was applied for c47 calculations. The structures of two conformers characterized by different orientations of ethyls in diethylamino substituent were optimized at B3LYP/6-31+G(d,p) level. The gas-phase absorption spectra were calculated at different levels of theory (CIS/def2-TZVPP, CIS/aug-cc-pvDZ CIS/6-31+G(d,p), TD DFT (PBE0/6-31+G(d,p)), CC2/def2-TZVPP CC2/aug-cc-pvDZ). Factor 0,72 [12] was used to scale the results calculated with CIS method. Maximum absorption wavelength, solvatochromic shift and dynamic Stokes shift were evaluated as described in the previous subsection. Additionally static Stokes shift was estimated as the difference between the excitation energies calculated within the non-equilibrium approach and the emission energies calculated by using the equilibrium solutions. Calculations were performed at TD PBE0/6-31+G(d,p) level. Supplementary optimizations were performed on ground and excited state geometries at DFT (PBE0 functional) and CC2 levels. Basis sets 6-31+G(d,p) and aug-cc-pvDZ were used for these calculations. Ground state and excited state dipole moments were evaluated at different levels of theory: CIS/6-31+G(d,p) , TD PBE0/6-31+G(d,p), TD-PBE0/aug-cc-pvDZ and CC2/aug-cc-pvDZ. The dipole moment calculations were carried out using GAUSSIAN09.

A cavity model was proposed for coumarin47/ $\beta$ CD complex. It was built on the HCTH optimized geometry of the complex. The cavity was constructed to replace the  $\beta$ CD. Twelve dummy atoms were placed at the distance  $d = 5,36 \text{ \AA}$  from the  $\beta$ CD mean axis in cylindrical arrangement, six on both sides of  $\beta$ CD mean plane at the distance  $l = 1,5 \text{ \AA}$ . The van der Waals radius on the dummy atoms was increased stepwise from  $r = 2,8 \text{ \AA}$  up to  $r = 4,2 \text{ \AA}$ . Corresponding absorption maximum and dipole moment of coumarin 47 in the cavity were estimated. Calculations were performed in Gaussian09. The solvent effects of water were included using PCM.

## 2 Results and discussion

### 2.1 $\beta$ -cyclodextrin-coumarin complexes

Gas-phase geometry optimizations were performed using PM3 and DFT (HCTH/6-31G, PBE0/6-31G, B3LYP/6-31+G(d,p)) methods. Due to the computational demands the complex geometry was optimized only at PM3 and HCTH/6-31G levels.

No significant changes concerning the bond lengths arose upon complexation. Differences in the coumarin geometry were mainly due the bond angles changes. Gas phase optimizations revealed planar structure of coumarin molecules. Slight distortion in the planarity of the coumarin moiety after encapsulation was observed at both levels of theory. In case of PM3 optimized complex with c522 the geometry of coumarin moiety became "twisted". This indicates that the PM3 method did not describe dispersion interactions properly.

Three of coumarins in our study contain diethylamino substituent. The PM3 optimization yielded geometries with pyramidalized nitrogen atoms for c6 and c30 in gas-phase and in complex. The originally planar structure of c47 changed to pyramidalized after the complex formation. In contrary, optimizations at DFT level estimated almost planar structure for N in diethylamino group for coumarins before and after the encapsulation.

The PM3 optimization of coumarin 522 yielded planar structure for the coumarin moiety distorted on the piperidine moiety. The geometry optimization performed with the same basis set (6-31G and 6-31+G(d,p)) yielded almost identical structures independent on the functional (PBE0 and B3LYP). The 6-31G optimizations yielded planar structures with the exception of C in piperidine and small pyramidalization angle on N. After the 6-31+G(d,p) optimization the planarity was distorted on the whole piperidine moiety. Simultaneously the pyramidalization angle of N(12) increased. The "twist" of coumarin moiety was widespread to the piperidine moiety. These results show that the 6-31G basis set overestimated the stability of coumarin molecule by spreading the  $\pi$  conjugation over the piperidine moiety.

In case of c6 and c 30 results of all optimizations confirmed planar benzothiazole and benzoimidazole moieties. Since these substituents were located outside the  $\beta$ CD cavity, their geometry had not changed upon complexation. The relative position of the substituent and coumarin moiety changed by rotating the substituent along the bond connecting them.

The PM3 gas-phase optimization of  $\beta$ CD yielded symmetric structure of the molecule. After the optimization with HCTH/6-31G the symmetry of  $\beta$ CD increased. The conical shape of  $\beta$ CD became more cylindrical and simultaneously the number of stabilizing hydrogen bonds increased. The structure of  $\beta$ CD upon complexation calculated with PM3 changed only slightly and the general shape remained the same. The HCTH optimizations led to deformation in the  $\beta$ CD symmetry. The gas phase symmetrical arrangement of glucose units became distorted by adopting the cavity to the shape of the inserted coumarin molecule. Intermolecular hydrogen bonds were observed in complexes except for c6.

The complexation energy was favourable for the complex formation for all coumarins. Our calculations were carried out without solvent. Due to the hydrophobicity of coumarins it can be expected that the presence of polar solvent will further increase the complex stability. The lowest complexation energy and the most pronounced deformation of coumarin and  $\beta$ CD in complex with c 522 (for coumarin at PM3 level and for  $\beta$ CD at DFT level) indicated that the complex formation with c30, c6 and c47 is more likely than in the case of c522.

HCTH optimized complexes and coumarins were used for spectra calculation at different levels of theory. Since the HCTH/6-31G was used to obtain the structures TD HCTH/6-31G was the first method applied. However, the absorption maxima of gas-phase coumarins were significantly overestimated and it completely failed in spectra calculation for  $\beta$ CD-coumarin complexes. Therefore, we estimated the shift due to the complex formation by TD PBE0/6-31G and CIS/6-31G. Since the CIS values were underestimated we scaled them by factor 0,72 [12]. Both methods agreed qualitatively well.

Upon encapsulation of coumarin in  $\beta$ CD red shift ( $\Delta\lambda_{\text{cmplx}}$ ) was observed for c47, c6 and c522. In contrary, the c30 absorption maximum was blue shifted. To see the origin for this effect we estimated the spectra of gas-phase coumarin in the geometry corresponding to that in complex. This calculation revealed that the shift due to the geometry difference ( $\Delta\lambda_{\text{geom}}$ ) for c30 was in opposite direction compared to other coumarins. The shift  $\Delta\lambda_{\text{geom}}$  was small for c47 and c522 since these are relatively small and rigid molecules in comparison to c6 and c30 and their geometry changed only slightly after the encapsulation. In case of c6 the most significant difference in geometry after encapsulation was enhanced planarity of the molecule. The resulting extension of  $\pi$  electron system caused red shift  $\Delta\lambda_{\text{geom}} = 6,68$  nm. The shift due to  $\beta$ CD presence ( $\Delta\lambda_{\text{cmplx}} - \Delta\lambda_{\text{geom}}$ ) was always red and approximately 10 nm for c6, c30 and c47. For c 522 the shift was the most pronounced. It seems likely that the size of the  $\beta$ CD cavity did not facilitate the inclusion of c552 in comparison to other coumarins. Thus the overall shift due to the complexation was a combination of above mentioned contributions ( $\Delta\lambda_{\text{geom}}$  and  $\Delta\lambda_{\beta\text{CD}}$ ) and could be in both directions according to the substituent groups on coumarins and the extent of geometrical changes on involved molecules upon inclusion.

The absorption spectra on B3LYP/6-31+G(d,p) geometry were calculated using PBE0 functional with two different basis sets, namely 6-31+G(d,p) and def2-TZVPP. Additionally, the absorption maxima were evaluated at CC2/aug-cc-pvDZ and CC2/def2-TZVPP levels for the two smaller coumarin molecules (c522, c47). The value of CC2/def2-TZVPP maximum absorption wavelength was used as a reference value to estimate the accuracy of PBE0 functional.

The results showed that even though the PBE0/6-31+G(d,p) put the lowest demand on computational time it still provided results with satisfactory accuracy in comparison to higher level theory calculations.

## 2.2 Benchmark study on coumarin 153

As a benchmark molecule for our spectra calculations we used coumarin 153 (Fig. 2e) . We have chosen this molecule because due to its simple solvatochromic behaviour it is often used as a solvation dynamics probe in experimental studies. We used the results published by Maroncelli et al. [13] as a benchmark data. It lists the values of solvent properties like dipole moments, dielectric constant, polarity scales and the absorption and emission frequencies and time dependent Stokes shift for C153 in number of solvents. Comparison of the experimental results with our calculated values presents a test study of the ability of theoretical methods to predict the solvatochromic behaviour of coumarin molecules in solvents of interest.

We compared the values of our calculated gas-phase maximum absorption wavelength to the experimental one from reference [14]. Our calculated values were  $27250\text{ cm}^{-1}$  and  $27038\text{ cm}^{-1}$  for 6-31+G(d,p) and def2-TZVPP basis set calculation, respectively. The corresponding CC2 value, using def2-TZVPP basis was  $26828\text{ cm}^{-1}$  and  $26617\text{ cm}^{-1}$  for aug-cc-pvDZ basis set. All calculated absorption maxima were in reasonable agreement with the experimental value  $27150\text{ cm}^{-1}$ . Comparison of gas-phase absorption wavelength showed that the gas phase calculations provide results directly comparable to the absolute values of experimental absorption wavelengths. Both basis sets with given functional yielded excellent results for gas phase absorption spectra.

We used PCM calculation to estimate the absorption wavelengths of coumarin 153 in various solvents. Addition of solvent effect through PCM caused red shift for all of the solvents. Noticeably the calculated absorption maxima differed systematically for the two used basis sets (6-31+G(d,p) and def2-TZVPP) by approximately  $200\text{ cm}^{-1}$  (Fig. 3). Apart from this small shift the use of different basis set appeared to have minor effect on the absorption spectra. The correlation factor of experimental and theoretical values was slightly better for the 6-31+G(d,p) basis set ( $R^2 = 0,71$ ) in comparison to def2-TZVPP basis set ( $R^2 = 0,69$ ).

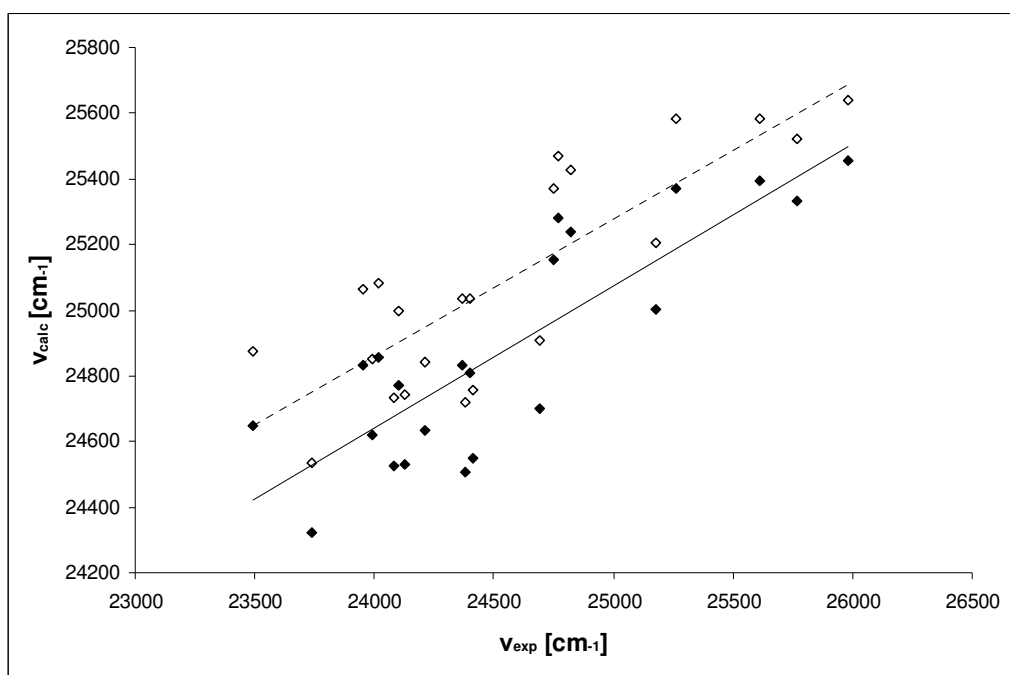


Fig. 3 Comparison of calculated ( $\blacklozenge$  PBE0/6-31+G(d,p),  $\diamond$  PBE0/def2-TZVPP) and experimental [13] values [ $\text{cm}^{-1}$ ] of maximum absorption wavenumbers  $\nu_{calc}$  and  $\nu_{exp}$ , respectively. Solid line is the fit of PBE0/6-31+G(d,p) data ( $\text{slope} = 0,43$ ,  $R^2 = 0,71$ ), dashed line is the fit of PBE0/def2-TZVPP data ( $\text{slope} = 0,42$ ,  $R^2 = 0,69$ ).

We estimated the solvatochromic shift from a nonpolar solvent (in this case cyclohexane) for theoretical and experimental absorption maxima. The correlation between experimental and calculated values is shown on Fig. 4. The shown absorption wavenumbers were obtained using 6-31+G(d,p) basis set. The results for TZVPP basis set differed only very slightly. The calculated shift was approximately one half (0,41) of the experimental shift but there was good qualitative agreement. The correlation factor of 0,71 has been very promising considering that we compared experimental values to theoretical values calculated using simplified solvation model. The above presented results showed that the PCM could be used to predict the absorption spectra in solvents. Although it underestimated the differences between solvents with various polarity the overall trend in the shift agreed with experimental one qualitatively well.

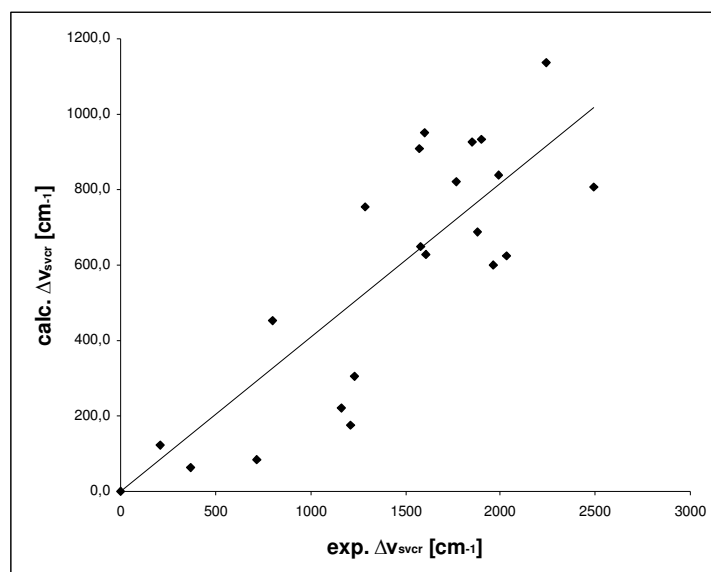


Fig. 4 Comparison of theoretically (PBE0/6-31+G(d,p)) and experimentally [13] estimated solvatochromic shift from cyclohexane  $\Delta\nu_{svcr}$  [ $\text{cm}^{-1}$ ]. The line represents the correlation of data ( $\text{slope} = 0,41$ ,  $R^2 = 0,71$ ).

Along with solvatochromic shift dynamic Stokes shift  $\Delta\nu_{dss}$  is another important aspect of solvatochromic behaviour. Fig. 5 represents a correlation plot of experimental measurements vs. calculated values. Clearly, most of the solvents followed the trend of linear correlation between experimental and theoretical values.

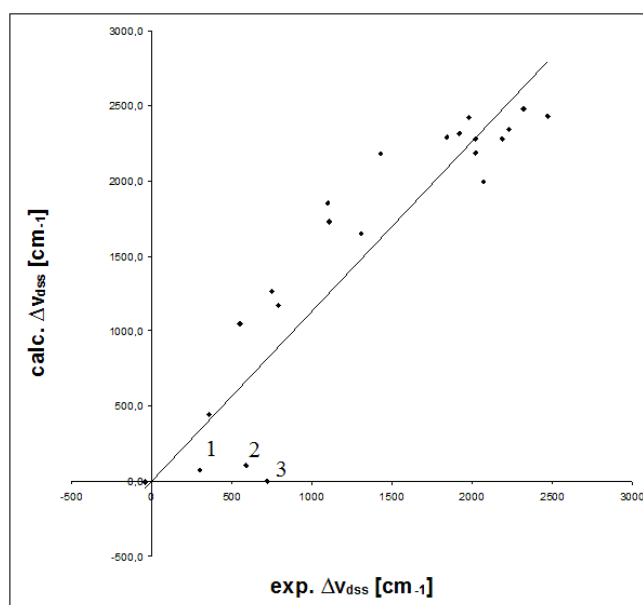


Fig. 5 Comparison of theoretically (PBE0/6-31+G(d,p)) and experimentally [13] estimated dynamic Stokes shift  $\Delta\nu_{dss}$  [ $\text{cm}^{-1}$ ]. The line represents the correlation of data ( $\text{slope}=1,13$ ,  $R^2=0,82$ ). (1 -  $\text{CCl}_4$ , 2 - toluene, 3 - benzene).

According to the physical effects involved in solvation of C153 the solvents can be distinguished into three categories. The first one presents dipolar solvents together with hydrocarbon solvents. Since the interactions between the solute and this class of solvents involve mainly the solute - solvent dipole interactions they are properly described by the continuum dielectric model.

The second class can be characterized as hydrogen-bond donating solvents. Even though the polarizable continuum model does not account for hydrogen bonds, the data revealed that this drawback plays negligible role in the shift. Following consideration can stress this point. Since the S0 - S1 transition in C153 is dominated by the  $\pi - \pi^*$  redistribution of electron density the  $\sigma$  electron density localised on the hydrogen bonds does not affect the transition. Moreover, already performed studies on C153 in protic solvents concluded that specific H-bonding interaction do not play a significant role in the spectral shifts of 153 [13,15].

Thus theoretical description of these two categories with PCM model reports the dominant features of interactions between solvent and solute and the results show good correlation with the experiment.

However, the third category of solvents shows underestimation of solvent induced shift by theoretical calculations. According to [13] these solvents can be described as "nondipolar". These solvents are ones that, by virtue of exact or near symmetry, have dipole moments that are exactly or approximately zero, but which nevertheless contain bonds that are expected to be significantly polar. The electrostatic interaction of solute are with the quadrupole and higher-order multipole moments of solvent molecules. While they are not directly reflected in the solvent's dielectric properties, they are by no means negligible compared to dipole-dipole interactions [13]. Theoretical models which fail to describe these interactions and gives values of  $\Delta V_{\text{dss}}$  that are not consistent with experimentally estimated Stokes shift. In our study this concerns the labelled points in Fig. 5 (1 - CCl<sub>4</sub>, 2 - toluene, 3 - benzene). Clearly the values of dynamic Stokes shift in these three solvents did not follow the overall trend. Keeping this in mind, calculated dynamic Stokes shift values were in excellent agreement with experiment.

Calculated dipole moment values for ground state and excited state are listed in Tab. 1. In ref. [15] only the value of ground and excited state dipole moment difference was discussed. The value reported is 4,1 D for spherical cavity with radius estimated from the van der Waals volume of C153. The CIS value  $\Delta\mu = 3,88$  would be in agreement with this value. However, this value was found to be overestimated by dielectric and electrochromic

measurements which yielded  $\Delta\mu = 7,5 - 9,5$  D. Also, in the paper published by Maroncelli et al. year later [13] the  $\Delta\mu$  value is estimated to 8D. In order to obtain more reasonable estimate radius depending on actual solvent and solute radii was chosen by Maroncelli et. al in ref. [15] and the predicted change in dipole moment was increased to 7,5 D. Our CC2 value (7,58 D) is in perfect agreement with this value. Even though the TD PBE0 calculation estimates  $\Delta\mu$  in better agreement with the actual value than CIS it still underestimates the dipole moment in excited state which leads to lower accuracy.

Method	Ground state $\mu$ [D]	Excited state $\mu$ [D]	$\alpha$ [deg]	$\Delta\mu$ [D]
CIS/6-31+G(d,p)	7,33	11,21	5,67	3,88
TD PBE0/6-31+G(d,p)	7,79	13,9	7,31	6,11
CC2/aug-cc-pvDZ	7,43	15,01	5,73	7,58

Tab. 1 Calculated dipole moments  $\mu$  in ground state and excited state [D], the angle  $\alpha$  between the ground and excited state dipole moment [deg], the change in magnitude  $\Delta\mu$  between ground and excited state dipole moments [D].

### 2.3 Spectral properties of coumarin 47

Our next molecule of interest was coumarin 47. The calculations were performed on two conformers of 47, A and B, which differ in the conformation of the diethylamine substituent. The terminal methyl groups of diethylamine outstand the coumarin mean plane, one above, the other beneath the mean plane for conformer A. In the case of B conformer the ethyl groups are in parallel alignment. Both conformers were optimized using B3LYP/6-31+G(d,p) in vacuum and the optimized structures were used for all absorption spectra calculation. The energy gap between these two conformers is 0,028 eV with A being the lower one. We used different methods (CIS, TD DFT, CC2) and different basis sets (def2-TZVPP, aug-cc-pvDZ, 6-31+G(d,p) ) for the absorption spectra calculation of C47 in vacuum. Values of gas-phase absorption maxima for both conformers are provided in Tab. 2.

Due to the lack of dynamical electron correlation, the scaling factor 0,72 proposed by Broo and Holmen [12] was used to scale the results obtained by CIS method. The scaled values are reported in parenthesis. In the absence of experimental data we take the CC2/def2-TZVPP value as a reference, since the basis set incompleteness error of def2-TZVPP basis set is small enough to obtain quantitative results at CC2 level. Noticeably, the DFT calculations

with the lowest basis set yielded absorption wavelengths near the actual CC2/def2-TZVPP values at considerably lower computational cost.

Method	$\nu_{\text{abs}} [\text{cm}^{-1}]$	
	Conformer A	Conformer B
CIS/def2-TZVPP	39110,8 (28159,77)	39133,46 (28176,09)
CIS/aug-cc-pvDZ	38764,0 (27910,08)	38782,2 (27923,18)
CIS/6-31+G(d,p)	39148,14 (28186,66)	39165 (28198,8)
TD DFT (PBE0/6-31+G(d,p) )	30286,51	30346,25
CC2/def2-TZVPP	30585,3	30677,9
CC2/aug-cc-pvDZ	30294,9	30357,7

Tab. 2 Gas phase maximum absorption wavelength of coumarin 47 for conformers A and B. For CIS calculation the scaled values are reported in parenthesis.

To get the insight into the influence of solvent on the C47 molecule absorption spectra in various solvents were calculated. In this work we used three different data sets published in ref. [16] (in this work referred to as *exp1*), in [17] (*exp2*) and [18] (*exp3*) for comparison of experimental and theoretical results. To see the influence of various solvents on the absorption spectra we use a plot of these versus reaction field factor. The results are shown on Fig. 6.

Alike in case of vacuum absorption spectra the shift between the A and B conformer was small. Therefore we focused only on the more populated A conformer. The values of TDDFT maximum absorption wavelength were overestimated in comparison to experimental values, but the overall trend of the results was satisfactory. The slopes of the fitting lines varied significantly even for the experimental data being -2109 for *exp1*, -1146 for *exp2* and -1841 for *exp3*. Our from DFT calculation estimated value -1552 was in good agreement with those from experiments. The unscaled results showed expected high overestimation of the absorption wavelength. Although the scaled values were closer to experimental data compared to DFT and the trend for the CIS results was correctly reproduced the very narrow slope (slope=-245 for scaled CIS) suggested that this method showed only slight sensitivity to different polarity of the solvents.

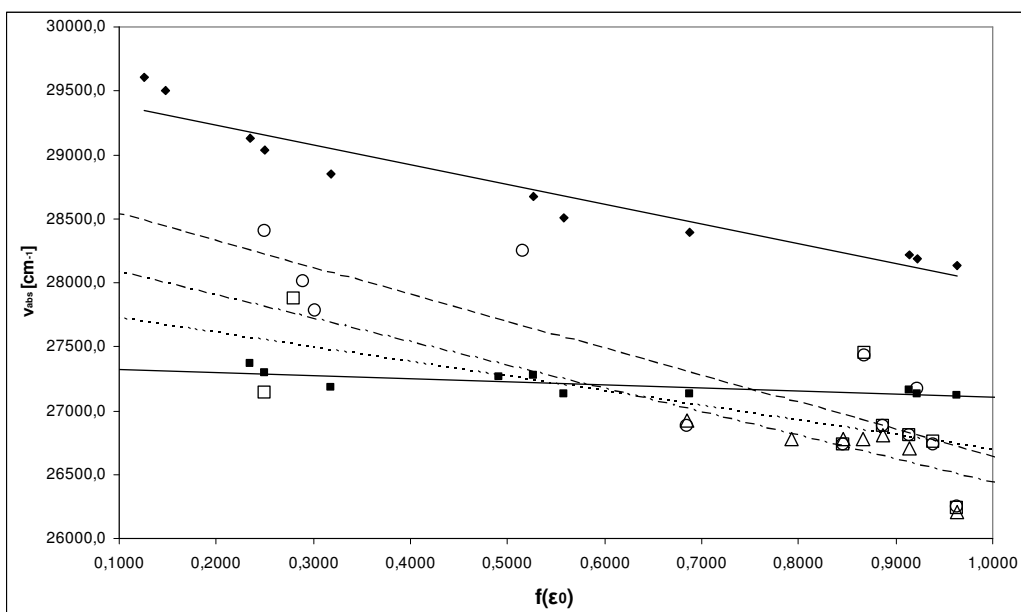


Fig. 6 Maximum absorption wavelengths  $\nu_{\text{abs}}$  of c47 in various solvents versus the reaction field factor  $f(\epsilon_0)$ . ( $\blacklozenge$  TDDFT,  $\blacksquare$  scaled CIS,  $\circ$  *exp1*,  $\square$  *exp2*,  $\triangle$  *exp3*, solid lines represent fits for theoretical data, long-dashed line for *exp1*, dotted line for *exp2*, dotted and dashed line for *exp3*)

The experimental Stokes shift for molecule in solution can be divided in static Stokes shift resulting from atomic relaxation of solute and dynamic Stokes shift arising due to the reorganization of solvent molecules in the environment of excited molecule. In spite of the simplicity of this model it captures two basic physical processes during the molecular excitation and deexcitation in solvent.

General trend of increasing Stokes shift with increasing solvent polarity was obvious and has been well reported by the theoretical results (Fig. 7). However, the slope of the correlation line (4855,2) was overestimated in comparison to experiments (1745,7 for *exp1*, 1380,3 for *exp2* and 3809,2 for *exp3*). As was already stated by C153 the absence of hydrogen bonding in PCM does not play any significant drawback when dealing with protic solvents. Therefore, it is no likely that the overestimation of the slope could be ascribed to missing hydrogen bonding in theoretical approach. Moreover, the interactions in alcoholic solvents are dominated by electrostatic interaction which are correctly described by PCM. On the other hand, the description of repulsion and dispersion interactions which outweighs the electrostatic interactions in less polar solvents is merely semiempirical. Additionally, these calculation were performed on the ground state geometry. Significant difference of excited state geometry would cause more pronounced shift in the emission spectra.

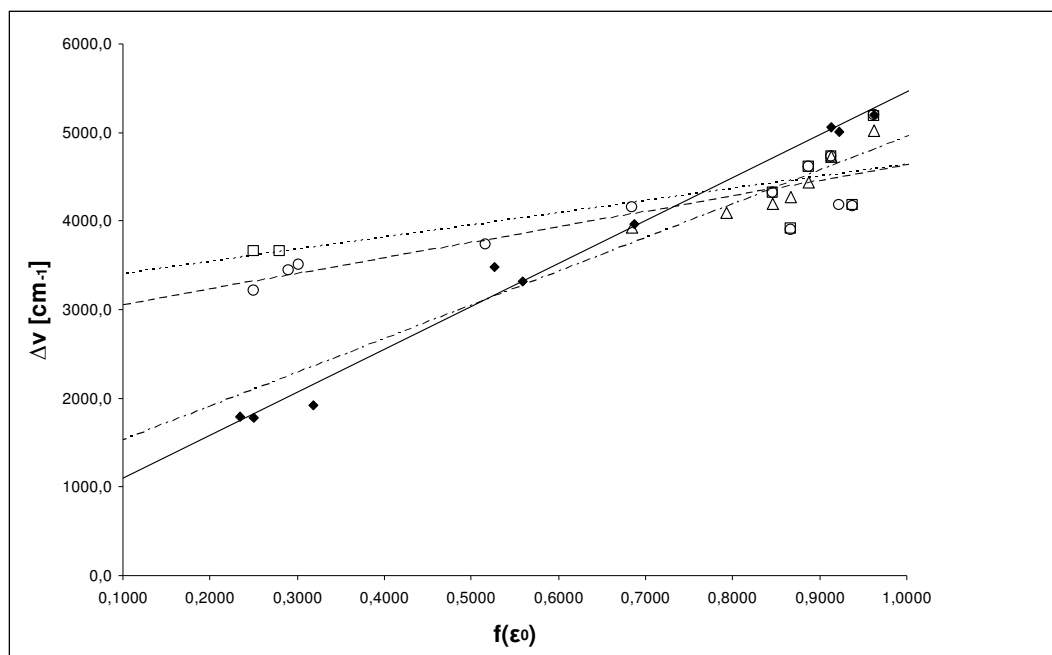


Fig. 7 Theoretically and experimentally estimated Stokes shift in solvents vs. the reaction field factor  $f(\epsilon_0)$ . ( $\blacklozenge$  TDDFT,  $\circ$  *exp1*,  $\square$  *exp2*,  $\triangle$  *exp3*, solid line represents fit for theoretical data, long-dashed line for *exp1*, dotted line for *exp2*, dotted and dashed line for *exp3*)

Therefore, we performed additional ground state (GS) and excited state (ES) optimizations at TD DFT and CC2 level of theory method with various basis sets (PBE0/6-31+G(d,p) and aug-cc-pvDZ). Using different basis set showed to have minor effect on the bond lengths. However using different method changed the geometry. In general the differences in the bond lengths were the largest in the pyran ring. By calculation at TD DFT level the geometry of the first excited state was close to the ground state structure. The second excited state was characterized by rotation of the diethylamino substituent. This structure was estimated in the first excited state at CC2 level of theory. The energy gap between the first ES and second ES conformation calculated at TD DFT level was only 0,02 eV. Therefore the difference between the ground and excited state geometry could be underestimated by calculations at TD DFT level. Moreover, experimental results showed that the polar solvents stabilize the non-emissive TICT [9,20] (or alternative radiationless deactivation - ULM [18]). With respect to this and the CC2 optimized excited state geometry we reviewed the Stokes shift vs. the reaction field factor plot (Fig. 7). If TD DFT could describe the emission of c47 in polar solvents properly the fit for theoretical data (solid line in Fig. 7) could be characterized by smaller slope value. Although the absorption maxima would be underestimated, the results could be in better qualitative agreement with experimental results.

Ground and excited state dipole moments calculated at different levels of theory are reported in Tab. 3.

Method	Ground state [D]	Excited state <sup>b</sup> [D]	Angle [deg.]
CIS/6-31+G(d,p)	7,84	10,04 (10,04)	14
TD-PBE0/6-31+G(d,p)	7,56	12,31 (12,30)	19
TD-PBE0/aug-cc-pvDZ	7,386	11,99	18
CC2/aug-cc-pvDZ	7,05	12,87	26
experimental <sup>a</sup>	5,25	12,53	

Tab. 3 Ground and excited state dipole moments, the angle between the ground and excited state dipole moments. <sup>a</sup>Experimental values taken from ref. [19]. <sup>b</sup>Values in parenthesis were evaluated manually.

The ES dipole moment calculated at TD DFT and CC2 level was in good agreement with the value of experiment. The lack of electron correlation involved in CIS led to underestimation of the ES dipole moment. All dipole moments in ground state were found to be overestimated in comparison to experimental value [19]. In theoretical study performed on coumarins 120 (which is structurally related to coumarin 47) by Cave et al. [21] they observed the same. They suggested that the experimental value of dipole moments in ground state by Nemkovich et al. [19] (used also in our study as reference) could be artificially low due to their methodology (neglect of polarizability contributions to the electrical response and assumption of collinear ground and excited state dipoles which was not confirmed in our study - see the angle between ground and excited state dipole moments in Tab. 3.) Additionally all calculations of ground state dipole moment carried out at different levels of theory yielded the value above 7D. These results indicated that the actual ground state dipole moment could be closer to our calculated values.

## 2.4 Cavity model

By encapsulation of coumarin in  $\beta$ CD the distance between the coumarin and solvent molecules increases. Thus the electrostatic interaction becomes weaker and the spectra of coumarin changes. In order to see the contribution of this effect on absorption spectra and dipole moment of c47 we proposed a cavity model of  $\beta$ CD-coumarin inclusion complex. The  $\beta$ CD was replaced by a cavity with free parameter which allowed us to vary the exposure of

c47 to the solvent environment. Thus the cavity simulated the  $\beta$ CD hydrophobic environment where no solvation of encapsulated coumarin molecule occurred.

To construct the model we first estimated the average distance  $d = 5,36 \text{ \AA}$  between the centroid of coumarin moiety of C47 and the glucose units of  $\beta$ CD. Then we placed 6 dummy atoms over and another 6 dummy atoms under the mean plane of  $\beta$ CD at the distance  $d$  from the coumarin mean axis. The distance between a pair of dummy atoms (one over, the other beneath the  $\beta$ CD mean plane) was  $3 \text{ \AA}$ . Fig. 8 shows coumarin 47 (carbon - green, oxygen - red) partially buried in the cavity (black). This model was built on the HCTH optimized geometry of complex. Absorption maximum wavelength and dipole moments were calculated at TD PBE0/6-31+G(d,p) level as a function of cavity parameter.

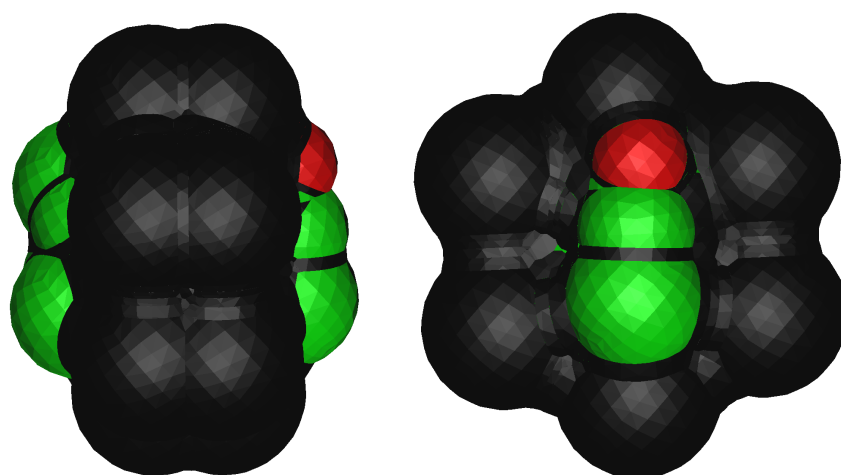


Fig. 8 Cavity model

By increasing the van der Waals radius on the dummy atoms the cavity was extended and the coumarin molecule became less solvated. Absorption maxima and the change in magnitude of dipole moment between ground state and excited state were calculated at different radii.

The cavity model together with spectral analysis of complex offer comprehensive outlook at spectral changes during the encapsulation of coumarin by  $\beta$ CD in solvent environment. To draw an inference on the overall spectral changes we use following consideration:

The cavity in our model should be approximately the same size as the van der Waals surface of  $\beta$ CD in PCM. From simple geometrical consideration, taking into account the distances of atoms in  $\beta$ CD and the UFF radii scaled by 1,1 used in PCM, we estimated the van der Waals radius on dummy atoms  $r = 3 \text{ \AA}$  as reasonable. By this value of  $r$  we obtained blue shift  $\Delta\lambda = 7,39 \text{ nm}$  resulting from the change in solvent environment of coumarin due to

encapsulation. Encapsulation itself produced red shift of the absorption maximum. The value was estimated to be  $\Delta\lambda = 7,86$  nm. Since both shifts (due to the complexation and the modification of solvent environment) were in opposite direction they would compensate each other. These results suggested that the absorption spectra of coumarin 47 in water solution and  $\beta$ CD-coumarin complex in water are very close. Therefore the original absorption maximum of coumarin, or small blue or red shift could be observed after the complexation. To the best of our knowledge there are no experimental studies on absorption spectra of  $\beta$ CD-coumarin 47 complex. However studies on other coumarins suggest that all these alternatives are possible for coumarin derivatives encapsulated in the  $\beta$ CD (no shift in study on coumarin [22], 5-8 nm blue shift in case of 7-diethylaminocoumarin-3-carboxylic acid [23], 4 nm red shift for c120 [24]). Thus even qualitative prediction of spectral change after complexation could be difficult. Nevertheless this model enables closer look at various contribution to the shift of absorption maxima upon complex formation.

### 3 Conclusions

In the present work we have explored structural and spectral properties of coumarin derivatives in various environments: in vacuum, in inclusion complexes with  $\beta$ CD and in solution.

The results showed that  $\beta$ CD was able to encapsulate coumarin molecules inside its cavity and that the complex formation was accompanied by geometrical changes. The complexes were stabilized by intermolecular hydrogen bonding. Calculations of maximum absorption wavelengths performed on gas-phase coumarins and complexes revealed that the shift between various geometry structures (gas-phase and that in the complex) can be either blue or red. The value of this shift depended on the rigidity of the molecule, substituent groups and depth of inclusion of particular coumarin molecule. Although the HCTH functional was used for geometry optimizations and provided reliable structures of  $\beta$ CD-coumarin complexes it failed in calculation of absorption maxima for the complexes.

The benchmark study on coumarin 153 and calculations on c47 confirmed the semi-quantitative reliability of TD DFT/PCM calculation with PBE0 functional for spectral properties evaluation. The general trend of more pronounced red shift with increasing solvent polarity was correctly reproduced with satisfying correlation factor. However, the theoretically evaluated solvatochromic shift was found to be underestimated in comparison

with experimental data. Calculated dynamic Stokes shift values for different solvents were in very good agreement with experimental data. Even though the PCM suffers on some shortcomings, like improper description of some class of solvents or general underestimation of solvatochromic shift, it is very powerful tool in understanding the effect of various solvents on given solute's spectra. The above presented result suggest that when aware of these shortcomings a conclusive comparison to experiment can be done. By comparison of the ground and excited state dipole moments to experimental counterparts we found that the TD DFT outperformed the CIS method and yielded values in good agreement with experiment and higher level theory.

The results obtained in course of our study and presented in this thesis suggest that DFT and TD DFT are useful for calculation of structural and spectral properties of coumarins. Implementation of solvent effects via PCM allows direct comparison of spectral properties to experimental results. The computational demands/accuracy ratio is reasonable for investigation of supramolecular complexes with  $\beta$ CD.

## References

- [1] Frisch, M. J.; Trucks, G. W.; Schlegel, H. B.; Scuseria, G. E.; Robb, M. A.; Cheeseman, J. R.; Montgomery, J. A., Jr.; Vreven, T.; Kudin, K. N.; Burant, J. C.; Millam, J. M.; Iyengar, S. S.; Tomasi, J. J.; Barone, V.; Mennucci, B.; Cossi, M.; Scalmani, G.; Rega, N.; Petersson, G. A.; Nakatsuji, H.; Hada, M.; Ehara, M.; Toyota, K.; Fukuda, R.; Hasegawa, J.; Ishida, M.; Nakajima, T.; Honda, Y.; Kitao, O.; Nakai, H.; Klene, M.; Li, X.; Knox, J. E.; Hratchian, H. P.; Cross, J. B.; Adamo, C.; Jaramillo, J.; Gomperts, R.; Stratmann, R. E.; Yazyev, O.; Austin, A. J.; Cammi, R.; Pomelli, C.; Ochterski, J. W.; Ayala, P. Y.; Morokuma, K.; Voth, A.; Salvador, P.; Dannenberg, J. J.; Zakrzewski, V. G.; Dapprich, S.; Daniels, A. D.; Strain, M. C.; Farkas, O.; Malick, D. K.; Rabuck, A. D.; Raghavachari, K.; Foresman, J. B.; Ortiz, J. V.; Cui, Q.; Baboul, A. G.; Clifford, S.; Cioslowski, J.; Stefanov, B. B.; Liu, G.; Liashenko, A.; Piskorz, P.; Komaromi, I.; Martin, R. L.; Fox, D. J.; Keith, T.; Al-Laham, M. A.; Peng, C. Y.; Nanayakkara, A.; Challacombe, M.; Gill, P. M. W.; Johnson, B.; Chen, W.; Wong, M. W.; Gonzalez, C.; Pople, J. A. Gaussian 03, Revision D. 02; Gaussian, Inc.: Wallingford, CT, 2004.
- [2] Allen F. H., *Acta Crystallogr.*, 2002, **58**(3), 380-388

- [3] HyperChem(TM) Professional 7.51, Hypercube, Inc., 1115 NW 4th Street, Gainesville, Florida 32601, USA
- [4] Stewart, J. J. P., *J. Comput. Chem.* 1989, **10**(2), 209–220.
- [5] Stewart, J. J. P., *J. Comput. Chem.* 1989, **10**(2), 221–264
- [6] Boese A. D., Handy N.C., *J. Chem. Phys.* 2001, **114**(13), 5497-6003
- [7] Adamo C., Barone V., *J. Chem. Phys.* 1999, **110**(13), 6158-6170
- [8] Becke A. D., *Phys. Rev. A.* 1988, **38**(6), 3098–3100
- [9] Lee C., Yang W., Parr R. G., *Phys. Rev. B.* 1988, **37**(2), 785-789
- [10] Becke A. D., *J. Chem. Phys.* 1993, **98**(7), 5648-5652
- [11] Tomasi J., Mennucci B., Cammi R., *Chem. Rev.* 2005, **105**(8), 2999–3094
- [12] Broo A., Holmén A., *Journal of Physical Chemistry A.* 1997, **101**(19), 3589-3600
- [13] Maroncelli M., Reynolds L., Horng M. L., Gardecki J. A., Frankland S. J. V., *Journal of Physical Chemistry.* 1996, **100**(24), 10337-10354.
- [14] Ernsting N. P., Asimov M., Schafer F. P., *Chem. Phys. Lett.*, 1982, **91**, 231. Source: Mennucci B., Ingrosso F., Tomasi J., *Journal of Molecular Liquids.* 2003, **108**(1-3), 21-46.
- [15] Maroncelli M., Horng M. L., Gardecki J. A., Papazyan A., *Journal of Physical Chemistry.* 1995, **99**(48), 17311-17337.
- [16] Zakerhamidi M.S., Ghanadzadeh A., Moghadam M., *Spectrochimica Acta - Part A: Molecular and Biomolecular Spectroscopy.* 2011, **78**(3), 961-966
- [17] Zakerhamidi M.S., Ghanadzadeh A., Tajalli H., Moghadam M., Jassas M., Hosseini Nia R., *Spectrochimica Acta - Part A: Molecular and Biomolecular Spectroscopy.* 2010, **77**(2), 337-341
- [18] López Arbeloa T., López Arbeloa F., Tapia M.J., López Arbeloa I., *Journal of Physical Chemistry.* 1993, **97**(18), 4704-4707
- [19] Nemkovich N.A., Reis H., Baumann W., *Journal of Luminescence.* 1997, **71**(4), 255-263
- [20] Kaholek M., Hrdlovič P., *Journal of Photochemistry and Photobiology A: Chemistry.* 1999, **127**(1-3), 45-55
- [21] Cave R.J., Burke K., Castner Jr. E.W., *Journal of Physical Chemistry A.* 2002, **106**(40), 9294-9305
- [22] Bakkialakshmi S., Menaka T., *Recent Research in Science and Technology.* 2010, **2**(5): 58-62

- [23] Tablet C., Matei I., Pincu E., Meltzer V., Hillebrand M., *Journal of Molecular Liquids*. 2012, **168**, 47–53
- [24] Nowakowska M., Smoluch M., Sendor D., *Journal of Inclusion Phenomena and Macrocyclic Chemistry*. 2001, **40**(3), 213-219

### Publikačná činnosť

AED01 Melicherčík, Milan, ml. 25% - Hianik, Tibor 25% - Holúbeková, Alžbeta 25% - Urban, Ján 25%: Effect of the model alpha-helical peptides on the structure of lipid bilayers - molecular dynamics simulations

Recenzované

Lit. 28 záz. n.

In: Acta Physica Universitatis Comenianae-New Series, Vol. 52. - Bratislava : Comenius University Press, 2011. - S. 41-47. - ISBN 978-80-223-3023-7

AEF01 Urban, Ján 15% - Mach, Pavel 15% - Babinec, Peter 14% - Masarik, Jozef 14% - Hubač, Ivan 14% - Holúbeková, Alžbeta - Malkin, Elena 14%: Studies of plasma wall with tungsten. Modelling of tungsten hydrogen complex

In: Annual Report of Association CU 2007. - Bratislava : Library and Publishing Centre, 2008. - S. 7-9. - ISBN 978-80-89186-39-6

POZNÁMKA: Vyšlo aj na CD ROM : Annual Report of Association CU 2007. -

Bratislava : Library and Publishing Centre, 2008. - S. 7-9. - ISBN 879-80-89186-40-2

AFG01 Holúbeková, Alžbeta - Mach, Pavel - Urban, Ján : Theoretical study of coumarine .BETA.-cyclodextrin inclusion complexes

In: 7th Southern School on Computational Chemistry and Materials Science. - Jackson : Jackson State University, 2007. - S. 47

[Computational Chemistry and Materials Science : Southern School. 7th, Jackson, 6.-7.4.2007]

## Zhrnutie

Metódou časovo závislej teórie funkcionálu hustoty sme skúmali štrukturálne a spektrálne vlastnosti derivátov kumarínu v rôznych prostrediach. Pre kumaríny 153 a 47 sme vypočítali maximá absorpčných spektier vo vákuu a v rôznych polárnych a nepolárnych rozpúšťadlách. Pri výpočtoch bol použitý funkcionál PBE0 v kombinácii s bázou 6-31+G(d,p). Vypočítané hodnoty posunu absorpčného maxima v rôznych rozpúšťadlách a dynamického Stokesovho posunu boli dobre porovnateľné s experimentálne určenými hodnotami. Porovnanie rozdielu medzi dipólovým momentom v základnom a v excitovanom stave ukázalo, že teoreticky určený rozdiel bol menší ako v prípade experimentov. Pri výpočtoch na vyššej úrovni (CC2) sa ukázalo, že za týmto rozdielom je nižšia hodnota excitovaného dipólového momentu pri výpočtoch metódou teórie funkcionálu hustoty. Výpočtami s použitím semiempirických metód (PM3) a metódou teórie funkcionálu hustoty (HCTH/6-31G) sme určili konformácie kumarínov 6, 30, 47, 522 a  $\beta$ -cyklodextrínu ( $\beta$ CD) v inklúznom komplexe. Vytvorenie komplexu sa z hľadiska komplexačnej energie javí ako výhodné. Enkapsulácia kumarínu v  $\beta$ CD a s tým spojené zmeny elektrónovej distribúcie mali za následok červený alebo modrý posun v spektre kumarínu. Preto sme navrhli model, v ktorom bol  $\beta$ CD nahradený kavitou. Tento model nám umožnil oddeliť rôzne príspevky k celkovému posunu spektra kumarínu pri vytvorení komplexu s  $\beta$ CD v rozpúšťadle.